Simultaneous two-photon imaging and photo-stimulation with structured light illumination

Marco Dal Maschio, Francesco Difato, Riccardo Beltramo, Axel Blau, Fabio Benfenati, and Tommaso Fellin*

Dept. of Neuroscience and Brain Technologies, Italian Institute of Technology, Via Morego 30, 16163 Genova, Italy
** tommaso.fellin@iit.it*

Abstract: Holographic microscopy is increasingly recognized as a promising tool for the study of the central nervous system. Here we present a "holographic module", a simple optical path that can be combined with commercial scanheads for simultaneous imaging and uncaging with structured two-photon light. The present microscope is coupled to two independently tunable lasers and has two principal configurations: holographic imaging combined with galvo-steered uncaging and holographic uncaging combined with conventional scanning imaging. We applied this flexible system for simultaneous two-photon imaging and photostimulation of neuronal cells with complex light patterns, opening new perspectives for the study of brain function *in situ* and *in vivo*.

OCIS codes: (090.1995) Digital holography; (180.2520) Fluorescence microscopy; (070.6120) Spatial light modulators; (180.4315) Nonlinear microscopy.

References and links

1. R. H. Kramer, D. L. Fortin, and D. Trauner, "New photochemical tools for controlling neuronal activity," Curr. Opin. Neurobiol. **19**(5), 544–552 (2009).
2. P. Saggau, "New methods and uses for fast optical scanning," Curr. Opin. Neurobiol. **16**(5), 543–550 (2006).
3. A. Bednarkiewicz, M. Bouhifd, and M. P. Whelan, "Digital micromirror device as a spatial illuminator for fluorescence lifetime and hyperspectral imaging," Appl. Opt. **47**(9), 1193–1199 (2008).
4. M. G. Gustafsson, L. Shao, P. M. Carlton, C. J. Wang, I. N. Golubovskaya, W. Z. Cande, D. A. Agard, and J. W. Sedat, "Three-dimensional resolution doubling in wide-field fluorescence microscopy by structured illumination," Biophys. J. **94**(12), 4957–4970 (2008).
5. B. E. Losavio, V. Iyer, and P. Saggau, "Two-photon microscope for multisite microphotolysis of caged neurotransmitters in acute brain slices," J. Biomed. Opt. **14**(6), 064033 (2009).
6. C. Lutz, T. S. Otis, V. DeSars, S. Charpak, D. A. DiGregorio, and V. Emiliani, "Holographic photolysis of caged neurotransmitters," Nat. Methods **5**(9), 821–827 (2008).
7. V. Nikolenko, B. O. Watson, R. Araya, A. Woodruff, D. S. Peterka, and R. Yuste, "SLM microscopy: scanless two-photon imaging and photostimulation with spatial light modulators," Front Neural Circuits **2**, 5 (2008).
8. T. L. Kelly, and J. Munch, "Phase-aberration correction with dual liquid-crystal spatial light modulators," Appl. Opt. **37**(22), 5184–5189 (1998).
9. K. D. Wulff, D. G. Cole, R. L. Clark, R. Dileonardo, J. Leach, J. Cooper, G. Gibson, and M. J. Padgett, "Aberration correction in holographic optical tweezers," Opt. Express **14**(9), 4170–4175 (2006).
10. D. R. Burnham, and D. McGloin, "Holographic optical trapping of aerosol droplets," Opt. Express **14**(9), 4176–4182 (2006).
11. D. Cojoc, F. Difato, E. Ferrari, R. B. Shahapure, J. Laishram, M. Righi, E. M. Di Fabrizio, V. Torre, and L. Mei, "Properties of the force exerted by filopodia and lamellipodia and the involvement of cytoskeletal components," PLoS ONE **2**(10), e1072 (2007).
12. M. Zahid, M. Vélez-Fort, E. Papagiakoumou, C. Ventalon, M. C. Angulo, V. Emiliani, and F. Tell, "Holographic photolysis for multiple cell stimulation in mouse hippocampal slices," PLoS ONE **5**(2), e9431 (2010).
13. N. Ji, H. Shroff, H. Zhong, and E. Betzig, "Advances in the speed and resolution of light microscopy," Curr. Opin. Neurobiol. **18**(6), 605–616 (2008).
14. G. Losi, K. Prybylowski, Z. Fu, J. H. Luo, and S. Vicini, "Silent synapses in developing cerebellar granule neurons," J. Neurophysiol. **87**(3), 1263–1270 (2002).
15. G. J. Brakenhoff, G. W. Wurpel, K. Jalink, L. Oomen, L. Brocks, and J. M. Zwier, "Characterization of sectioning fluorescence microscopy with thin uniform fluorescent layers: Sectioned Imaging Property or SIPcharts," J. Microsc. **219**(Pt 3), 122–132 (2005).

#128503 - $15.00 USD Received 26 May 2010; revised 29 Jul 2010; accepted 7 Aug 2010; published 18 Aug 2010

16. E. Papagiakoumou, V. de Sars, D. Oron, and V. Emiliani, "Patterned two-photon illumination by spatiotemporal shaping of ultrashort pulses," Opt. Express **16**(26), 22039–22047 (2008).
17. C. Maurer, S. Khan, S. Fassl, S. Bernet, and M. Ritsch-Marte, "Depth of field multiplexing in microscopy," Opt. Express **18**(3), 3023–3034 (2010).
18. G. Sinclair, J. Leach, P. Jordan, G. Gibson, E. Yao, Z. Laczik, M. Padgett, and J. Courtial, "Interactive application in holographic optical tweezers of a multi-plane Gerchberg-Saxton algorithm for three-dimensional light shaping," Opt. Express **12**(8), 1665–1670 (2004).
19. V. Emiliani, D. Cojoc, E. Ferrari, V. Garbin, C. Durieux, M. Coppey-Moisan, and E. Di Fabrizio, "Wave front engineering for microscopy of living cells," Opt. Express **13**(5), 1395–1405 (2005).
20. M. Fricke, and T. Nielsen, "Two-dimensional imaging without scanning by multifocal multiphoton microscopy," Appl. Opt. **44**(15), 2984–2988 (2005).

1. Introduction

A rapidly increasing number of new optical tools for the study of brain function is becoming available to neuroscientists. These tools include, among others, fluorescent and photo-switchable molecules, caged compounds, light-activated ion channels and pumps [1]. In parallel with the increasing size of this "optical toolbox" for brain circuit investigation, there is a growing need for optical techniques that allow the illumination of the biological sample with precise, yet complex, spatial patterns. For example, many applications require the fast/simultaneous monitoring/stimulation of different regions of interest (ROIs) in the field of view [2]. A number of different approaches including digital micromirror devices (DMDs), multibeam illumination, acusto optic deflectors (AODs) and liquid crystal on silicon spatial light modulators (LCOS-SLMs) have been developed to achieve this goal [3–7]. Among these, LCOS-SLMs, which shape the laser wave-front by modulating the phase of the incident light, are increasingly recognized as a very promising approach to generate structured light illumination.

LCOS-SLMs are composed of a high density matrix of liquid crystal pixels. By regulating the orientation of the liquid crystals within each pixel, it is possible to finely modulate the phase of the light impinging on the LCOS-SLM. The whole active area of a spatial light modulator can be configured via software with a diffractive optical element (DOE) which results in the desired pattern of illumination at the sample plane. The LCOS-SLMs generally have a limited diffraction efficiency compared to phase plates (about 40% vs 85%), and a lower refresh rate with respect to DMDs (180 frames/s *vs* 13 kframes/s). Nonetheless, LCOS-SLMs offer the opportunity to generate arbitrary DOEs using the whole numerical aperture of the objective, without affecting the total amount of light power delivered to the sample. Moreover, commercial LCOS-SLMs with proper optical windows covering the wavelengths ranging from UV to IR are readily available.

Initially used for aberration correction optics and optical-tweezer applications [8–11], holographic microscopy using LCOS-SLMs has been recently applied to functional studies of neuronal physiology with very encouraging results. Patterned uncaging of caged-glutamate in combination with electrophysiology has been performed in brain slice preparation either by using single [6] or two-photon excitation [7]. Fast glutamatergic currents of various amplitude and kinetics could be elicited by patterned light illumination of various neuronal structures including spines, portions of dendrites and cell bodies. Moreover, a very recent study extended these initial findings and combined single photon holographic uncaging with HiLo (high frequency/low frequency) sequential acquisition microscopy to study the response of neuronal and glial cells to glutamate photolysis in hippocampal slices [12]. Besides uncaging, holographic illumination with LCOS-SLMs has also been used for fast, scanless imaging of neuronal fluorescence signals [7], thus improving the time resolution of low invasive imaging techniques [13].

Despite these results show the potential of holographic microscopy for the investigation of neuronal circuits, this approach has still very limited diffusion in Neuroscience laboratories due to the lack of commercially available holographic microscopes and the need to develop customed, optical apparatus.

#128503 - $15.00 USD Received 26 May 2010; revised 29 Jul 2010; accepted 7 Aug 2010; published 18 Aug 2010

In this paper we present a "holographic module", a compact, simple optical path that can be easily implemented with commercial scanheads to allow spatial shaping of laser light. The combination of the holographic module with a Prairie Ultima IV scanhead (Prairie Technologies, Madison WI) constitutes a holographic microscope capable of simultaneous two-photon imaging and uncaging using two independent laser sources at different wavelengths. The present set-up gives the opportunity to combine the intrinsic three-dimensional spatial resolution of a non-linear imaging system with the possibility to simultaneously access arbitrary regions of the sample in time and space. We show that this microscope represents a flexible optical set-up with multiple experimental configurations that can be applied to the study of neuronal tissue. Given the enhanced tissue penetration depth of infrared radiation compared to visible light, this system opens new vistas in the application of holographic microscopy to the investigation of the central nervous system both *in situ* and *in vivo*.

2. Materials and methods

2.1 Optical setup

The optical set up is composed of two mode-locked Ti:Sapphire laser sources (one Ultra and one Ultra II Chameleon, Coherent, Milan, Italy), the "holographic module" (Fig. 1A-B, pink area), a commercial Prairie Ultima IV scanhead (Fig. 1A-B, blue area, Prairie, Madison, WI) and an upright epifluorescence microscope (BX61 Olympus, Milan, Italy).

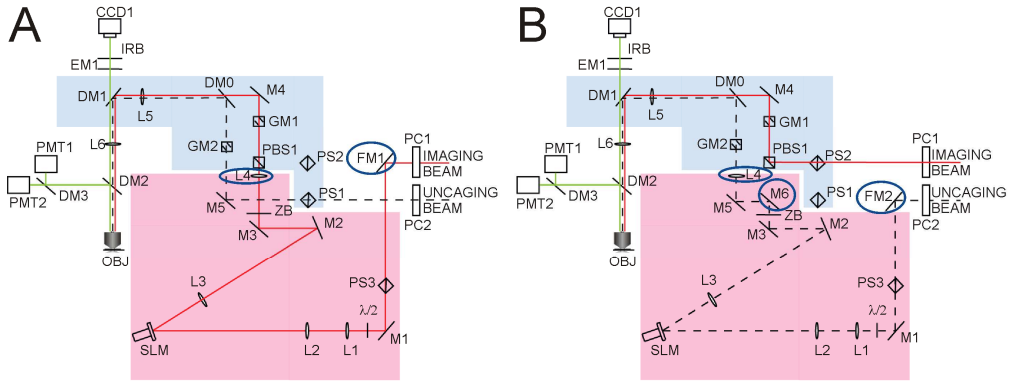

Fig. 1. Schematic representation of the two experimental configurations of the optical set-up. A) The imaging beam (solid red line) coming from a Coherent Ultra II Chameleon laser is deflected by a flipping mirror (FM1), reshaped and modulated by the "holographic module" (pink area of the optical layout) and then directed to a commercial Prairie Ultima IV scanhead (blue area of the optical layout) coupled with a motorized Olympus BX61 microscope. A first telescope (L1 and L2) is used to reshape the laser beam to fit the Hamamatsu LCOS-SLM active window, while the lenses L3 and L4 form a second telescope that optimizes the beam size according to the dimensions of the mirrors inside the scanhead. A half wave plate (λ/2) is placed before the LCOS-SLM to modulate the beam polarization (see Methods section). A small piece of aluminum foil (ZB) mounted on a glass coverslip is placed at the focal plane of the second telescope (between L3 and L4) to reflect the zero order light (see description of the optical set up in the main text). *Legend*: PC1, pockel cell of the imaging beam; PC2, pockel cell of the uncaging beam; M1, turning mirror; λ/2, half wave plate; L1, plano-convex lens (f = 30 mm); L2, plano-convex lens (f = 100 mm); SLM, spatial light modulator; L3, plano-convex lens (f = 300 mm); M2, turning mirror; M3, turning mirror; ZB, zero order block; L4, plano-convex lens (f = 100 mm); PBS1, polarizing beam splitter; GM1, galvo mirror of imaging beam; M4, turning mirror; DM0, 760 nm long-pass dichroic mirror; L5, proprietary scan lens (f = 75 mm); DM1, 660 nm short-pass dichroic mirror; L6, proprietary tube lens (f = 180 mm); DM2, 660 nm long-pass dichroic mirror; DM3, 575 nm long-pass dichroic mirror; PMT1, photomultiplier #1; PMT2, photomultiplier #2; CCD1, CCD camera; GM2, galvo mirror of the uncaging beam; OBJ, microscope objective. (B) The uncaging beam (dashed black line) coming from a Coherent Chameleon Ultra laser is deflected by a flipping mirror (FM2) in the

#128503 - $15.00 USD Received 26 May 2010; revised 29 Jul 2010; accepted 7 Aug 2010; published 18 Aug 2010

"holographic module". Beam path is the same as described in A) except that the laser light is deflected by a mirror (M6) into the uncaging pathway of the Prairie scanhead. The plano-convex lens L4 (f = 100 mm) is, in this experimental configuration, moved to the uncaging path. The blue circles point to the optical elements that are different between the configuration displayed in A) and that shown in B). *Legend*: FM2, flipping mirror; M6 turning mirror.

The "holographic module" is composed of seven principal parts: *i) Flipping mirrors* (FM1, FM2 in Fig. 1A-B, PF10-03-P01 Thorlabs, Newton, NJ). This couple of mirrors is used for deflecting either one or the other laser beam onto the holographic path. When structured illumination is desired in the imaging or uncaging paths, the flipping mirror FM1 or FM2 are flipped up respectively. Figure 1A shows the microscope in the configuration in which holographic illumination is performed in the imaging path (solid red line). Figure 1B shows the alternative configuration in which holographic illumination is applied to the uncaging beam (dashed black line), while the imaging beam (solid red line) is directed to the scanhead scanning mirrors. When no holographic illumination is required in either one of the laser beams, both flipping mirrors (FM1 and FM2) stay in the down position. *ii) Periscope*. A series of mirrors (PS3 in Fig. 1, BB1-E03 Thorlabs, Newton, NJ) is used to bring the light from the plane of the optical table to that of the input port of the scanhead. *iii) Half wave plate* (λ/2 in Fig. 1, RAC 5.2.10 achromatic λ/2 retarder - B. Halle Nachfl GMBH). The LCOS-SLM is sensitive to the polarization of the incident light. It acts as a phase-only modulator for light linearly polarized in the direction corresponding to the liquid crystal orientation. The half-wave plate has thus to be properly rotated in order to match the LCOS-SLM optimal orientation. *iv) Primary telescope*. A pair of plano-convex lenses (L1 and L2 in Fig. 1, IR doublets, Thorlabs, Newton, NJ) is used to resize the laser beam to fill the active window of the LCOS-SLM. Using this approach, we spread the beam power throughout the maximum number of pixels available on the LCOS-SLM chip, to exploit the highest frequency content of the computer-generated diffractive optical element (DOE). *v) LCOS-SLM*. We used a reflective X10468-07 LCOS-SLM (Hamamatsu, Milan, Italy) with the following characteristics: pixel resolution, 800x600; active area dimension, 16 x 12 mm^2; pixel dimension, 20x20 μm^2; wavelength range, 680-1100 nm; pixel fill factor, 95%; phase modulation, 0-2π; refresh rate, 60 Hz. The LCOS-SLM is controlled by means of a modified version of the open-source Labview-based software released by the Optics Group of the Physics Department of the University of Glasgow (http://www.physics.gla.ac.uk/Optics/projects/tweezers/software/; see section *2.2* for details) and interfaced with a computer via a DVI connection. With respect to the direction normal to the LCOS-SLM plane the reflective angle is 9.5°. *vi) Secondary telescope*. It reshapes the laser beam to fit the dimensions of the mirrors inside the scanhead conjugating the LCOS-SLM to the objective back focal plane. It is composed of two plano-convex lenses (L3 and L4 in Fig. 1A-B, IR doublets, Thorlabs, Newton, NJ). *vii) Zero order block*. To remove the straight light of the "zero order" component, a small piece of aluminum foil is mounted on a glass coverslip and placed at the Fourier plane of the first lens of the secondary telescope (ZB, between L3 and L4, see Fig. 1).

With the exception of the flipping mirrors (FM1 and FM2) and of the first mirror of the periscope, which are mounted on the optical table, all the remaining parts of the "holographic module" are mounted on a single breadboard elevated to the plane of the scanhead. The physical dimensions of the "holographic module" are: 60 x 30 x 18 cm^3 (L x W x H). We measured the broadening of femtosecond pulses at the sample plane with an Olympus 20X, objective and a CARPE autocorrelator (APEBerlin, Berlin, Germany). In the 760-980 nm range, the average group velocity dispersion (GVD) introduced by the "holographic module" is approximately 20000 fs^2.

The Ultima IV Prairie scanhead has two sets of galvo mirrors. GM1 in Fig. 1 are scanning mirrors for the imaging beam while GM2 are beam steering mirrors for the uncaging beam.

#128503 - $15.00 USD Received 26 May 2010; revised 29 Jul 2010; accepted 7 Aug 2010; published 18 Aug 2010

The two beams are then combined by a dichroic mirror DM0 and reshaped to match the pupil aperture of the microscope objective (L5 and L6 in Fig. 1A-B).

DM1 in Fig. 1 is a short-pass dichroic mirror (FF670-SDi01, Semrock) which reflects two-photon excitation light onto the sample and allows the detection of emitted fluorescence (green line in Fig. 1) via a CCD camera (ORCA R2 Hamamatsu, Milan, Italy). An IR blocking filter (ET750sp-2p8, Chroma) in combination with specific emission filters is positioned in front of the camera for fluorescence imaging. Alternatively, when traditional scanning fluorescence microscopy is required, the dichroic mirror DM2 is inserted in the emission path to deflect fluorescence signals to the two photomultipliers tubes (PMTs).

The switch between the configuration shown in Fig. 1A and that displayed in Fig. 1B is essentially limited to three steps (circled in blue in Fig. 1B), namely: 1) Turn down the flipping mirror (FM1) in the imaging path and turn up the flipping mirror (FM2) in the uncaging path. 2) Move the lens L4 of the secondary telescope from the imaging to the uncaging path. 3) Position the mirror M6 to deflect the holographic uncaging beam onto the uncaging galvos (GM2).

2.2 Generation of the diffractive optical element (DOE)

In order to generate appropriate DOEs, the SLM is controlled via personal computer by a modified version of the Labview-based software "Blue Tweezers" (released by the Optic Group, Department of Physics, University of Glasgow; http://www.physics.gla.ac.uk/Optics/projects/tweezers/software/). The modified software allows the calibration of the field of view in which holographic illumination can be performed ("holographic field") with respect to the fields of view of the image-acquisition devices (PMTs and CCD camera). Once this calibration procedure is performed, various regions of interest with arbitrary shapes can be defined based on the images acquired with the camera or with the PMTs, depending on the configuration used (Fig. 1A or Fig. 1B respectively). Images are transformed into binary masks and used as input matrices for the Gerchberg-Saxton algorithm adopted for the generation of the DOEs.

2.3 Neuronal cell preparation

All the experimental protocols were approved by the Italian Ministry of Health. Primary neuronal cultures from the hippocampus were prepared from neonatal E18 C57BL6/J mice. Blocks of tissue from the hippocampus were removed and chopped. Cells were dissociated in trypsin (0,125 mg/ml) and then placed on poly-D-lysine-coated (100 μg/ml; Sigma) glass coverslips at a density of $5x10^4$ cells per dish. Cells were incubated with Neurobasal medium supplemented with 10% fetal bovine serum, penicillin/streptomycin (10^4 units/ml penicillin; 10^4 μg/ml streptomycin) and glutamine (200 mM, Invitrogen, Milan, Italy). After three hours the medium was replaced with Neurobasal medium supplemented with B27 (Invitrogen, Milan, Italy), penicillin/streptomycin (10^4 units/ml penicillin; 10^4 μg/ml streptomycin) and glutamine (200 mM, Invitrogen, Milan, Italy). Cerebellar granule cells used for the experiments displayed in Fig. 6 were prepared as described in [14]. Cells were used at 10-15 days in vitro and incubated with 1.5 μM Fluo-4 for 30 minutes in HEPES buffered saline before recording. Fluo-4 fluorescence was excited at 830 nm and filtered by an emission filter (530/50 nm Chroma). MNI-glutamate (1.5 mM, Tocris, Bristol, UK) was added to the extracellular saline before performing the uncaging experiment.

3. Results

We first characterized the properties of the holographic optical path. As shown in Fig. 2, different holograms could be generated with the SLM on either the imaging or the uncaging lasers, resulting in complex patterns of illumination in the sample plane. We observed the shaping of the laser beam either by imaging the two-photon light reflected by a mirror positioned at the sample plane (Fig. 2C) or by measuring the fluorescence emitted by a

#128503 - $15.00 USD Received 26 May 2010; revised 29 Jul 2010; accepted 7 Aug 2010; published 18 Aug 2010

homogeneous 115 nm thick layer of fluorescein and perylenediimid (Fig. 2D) [15]. Multiple spots (Fig. 2, top) or arbitrary shapes of various dimensions (Fig. 2, middle and bottom) could be generated, resulting in the illumination of desired regions of interest (ROIs) in the field of view.

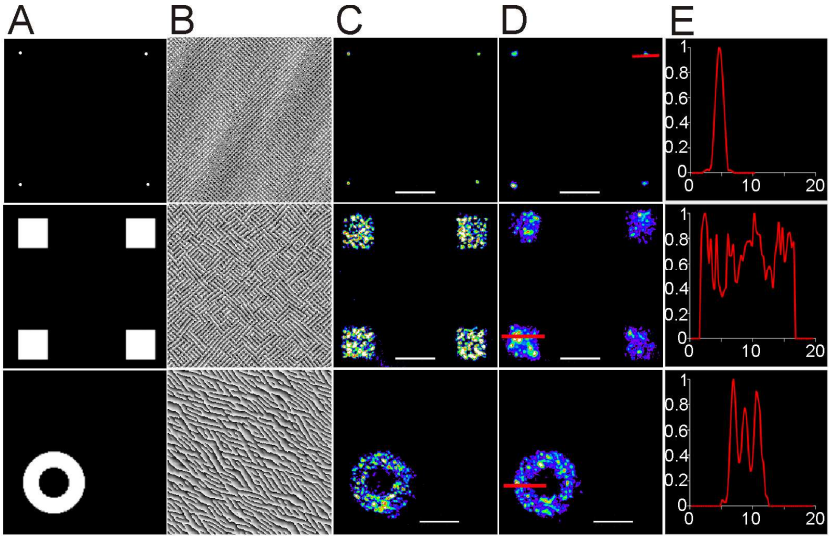

Fig. 2. Two-photon structured light illumination. A) Example of light patterns that can be projected onto the sample plane. Four diffraction-limited spots positioned at the four corners of the field of view (top image), four rectangular shapes (middle panel) and a donut-like shape (bottom image) are shown. (B) Computer-generated DOEs corresponding to the different light patterns shown in (A) are sent to the LCOS-SLM. Given that the LCOS-SLM is a phase-only modulator, black/white shades on the panel correspond to 0-2 π phase modulation. (C) Two-photon excitation light reflected by a mirror positioned in the focal plane of the objective measured for the different illumination patterns shown in (A). Scale bar 20 μm. (D) Fluorescence signals from a 115 nm thick layer of fluorescein and perylenediimid generated by the two-photon excitation patterns shown in (A). Scale bar 20 μm. These data were obtained with the instrument in the configuration shown in Fig. 1A but similar results were gathered when the uncaging laser was deflected into the "holographic module" (configuration shown in Fig. 1B). The objective used was an Olympus 20X. (E) Line profiles showing the variation of light within different holographic shapes. Profiles shown in E correspond to the red lines shown in (D). Values on the x axis are expressed in μm while the y axis shows normalized intensity values in arbitrary units.

The intensity profile of large spots was characterized by sharp edges with relatively large variation (~60% for a circular shape of 8 μm diameter) within the spot (see also Fig. 2E). Noteworthy, enlarging the spot size (Fig. 2, middle) decreased the density of photons in the imaged area but still maintained a sufficient two-photon excitation probability to induce fluorescence emission. We performed structured illumination with a number of different Olympus objectives from a 20X (XLUMPLFL20XW, 0.95 NA) to a 40X (LUMPLFL40XW, 0.8 NA) and a 60X (LUMFL, 1.1 NA). The area where holographic shaping of light could be achieved was a subregion of the field of view the dimensions of which depended on the objective used. For a 20X (0.95 NA) objective, which was mostly used to perform the experiments described in this study, the holographic field had a diameter of ~150 μm.

In our experimental configuration, approximately 29% of the incoming light went in the un-diffracted "zero order" component. As previously reported [7], for most experiments we adopted the configuration in which the zero order beam was in the center of the field of view and was blocked by a small reflecting piece of aluminum foil positioned in the Fourier plane of the first lens of the secondary telescope (see Fig. 1). This plane is conjugated to the plane of the sample and the removal of the zero order by reflection in the conjugated plane caused

#128503 - $15.00 USD Received 26 May 2010; revised 29 Jul 2010; accepted 7 Aug 2010; published 18 Aug 2010

the appearance of a negligible dark region (< 8 μm in radius) in the center of the field of view. Given that we have control of the relative position of the sample with respect to the holographic beam, this does not represent an experimental constraint. The holographic optical path, including the block of the "zero order" beam, had an overall transmission efficiency of about 40% resulting in a maximum power delivered to the sample of about 200 mW (at 720 nm). This value represents an upper limit to the number and size of holographic spots that could be generated in the field of view, given that this value of power had to be distributed between the different holographic shapes and that a certain amount of power (see also Fig. 5-6) was required to generate two-photon excitation/uncaging for each single holographic shape.

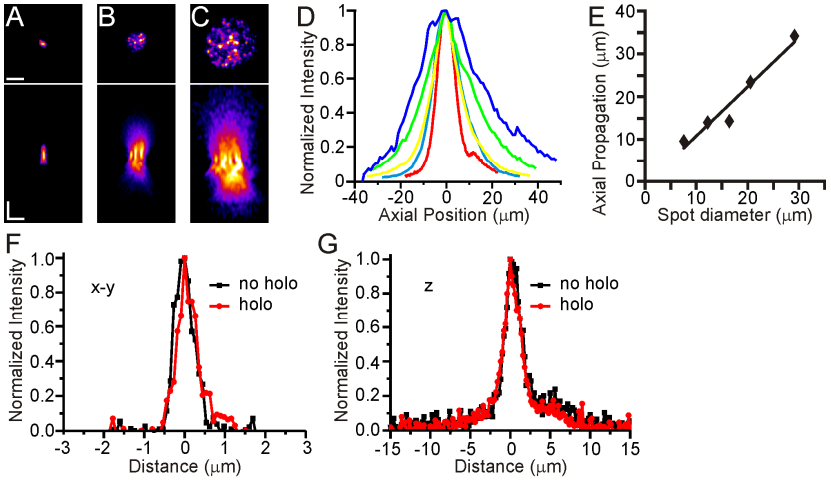

Fig. 3. Axial dimension of structured light and point spread function of the holographic microscope. A-C) x-y (top) and x-z (bottom) profiles for illumination of a 115 nm thick film of fluorescein and perylenediimid with three circular shapes of different diameter. Scale bars: 10 μm. D-E) The intensity profile in the axial direction is generated for five different patterns of illumination (D). The full width (in the axial direction) at half maximum (FWHM) is then measured and plotted as a function of the x dimension of the light pattern (E). Note that the x dimension is calculated as the width of the intensity profile (in the x direction) at a threshold level set to 5 times the standard deviation of the background. F-G) Intensity profiles in the x-y (F) and z (G) directions of sub-resolved (20 nm) fluorescent beads excited at 830 nm with the imaging beam passing (holo, red trace) and not passing (no holo, black trace) through the "holographic module". Each trace is the average of four measurements on different beads. These recordings were performed with a 60X, water immersion objective with a numerical aperture of 1.1.

We also characterized the axial dimension of the shaped beam. The axial propagation of circular shapes of different diameters is shown in Fig. 3A-D (images acquired with a 20X objective). As previously shown for single [6] and two-photon excitation [16], we confirmed the linear relationship between the x-y dimension of the holographic shape and the axial propagation (FWHM, Fig. 3E). Moreover, light impinging on different radial regions of the "holographic field" propagated similarly in the axial direction (data not shown). Importantly, the introduction of the "holographic module" did not significantly affect the point spread function (PSF) of the microscope (Fig. 3F-G).

We implemented our software to utilize images acquired either with the scanning two-photon system or with wide-field camera to generate the desired pattern of illumination (see method section 2.2). Once the two-photon or epifluorescence images were acquired, ROIs were generated, and used as a mask to create complex patterns of excitation in our sample plane according to the geometry of the biological sample. Figure 4A shows the epifluorescence image of a Fluo-4 loaded neuron. The image was then binarized (Fig. 4B-B_2) according to specific ROIs corresponding to different portions of the cell, and used to generate a phase hologram (Fig. 4C-C_2) to illuminate only the selected regions. Figure 4D-D_2 shows

#128503 - $15.00 USD Received 26 May 2010; revised 29 Jul 2010; accepted 7 Aug 2010; published 18 Aug 2010

the Fluo-4 fluorescence image obtained with holographic two-photon illumination according to the ROIs defined in Fig. 4B-B_2.

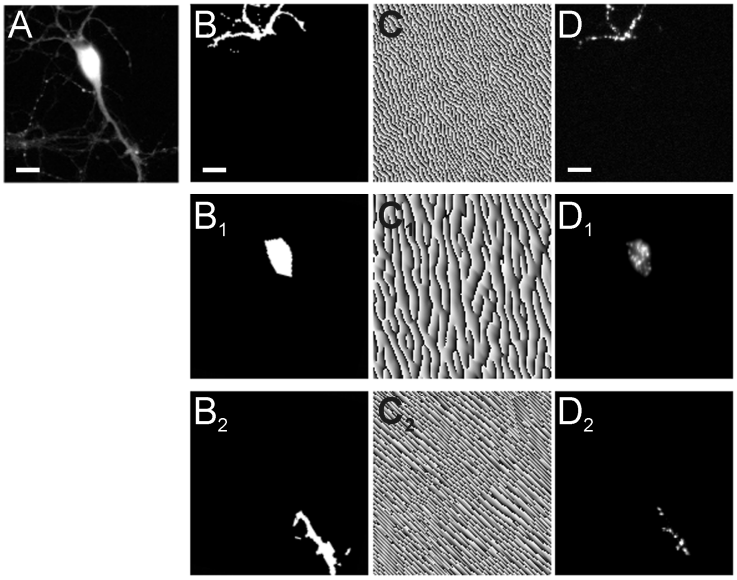

Fig. 4. Illumination of a neuronal cell with complex light patterns. A) A two-photon fluorescence image of a Fluo-4-loaded neuron is acquired with the CCD camera (CCD1 in Fig. 1). Scale bar: 10 µm. B-C) Binary images containing only the regions of interest corresponding to the cell body (B_1) or the neuronal processes (B and B_2) are created *a posteriori* from the image shown in (A) and used to generate the DOEs displayed in C-C_2). Scale bar: 10 µm. D-D_2) Fluorescence images obtained with holographic illumination with the patterns shown in (B-B_2). Scale bar: 10 µm.

To demonstrate the suitability of the presented holographic microscope for simultaneous two-photon imaging and uncaging on living cells in the two experimental configurations described in Fig. 1, we measured cytosolic Ca^{2+} signals in neuronal cultures while uncaging MNI-glutamate. We first used the experimental configuration in which holographic imaging is combined with galvo-steered uncaging (Fig. 1A). An image of Fluo-4 fluorescence (Fig. 5A) was first acquired with the two-photon scanning system and used to generate a desired DOE. The DOE shaped the imaging beam to illuminate only specific ROIs in the field of view corresponding to different cells or different portions of a given cell (nine green spots in Fig. 5A; average power of the imaging laser/spot, < 4 mW; λ = 830 nm).

#128503 - $15.00 USD Received 26 May 2010; revised 29 Jul 2010; accepted 7 Aug 2010; published 18 Aug 2010

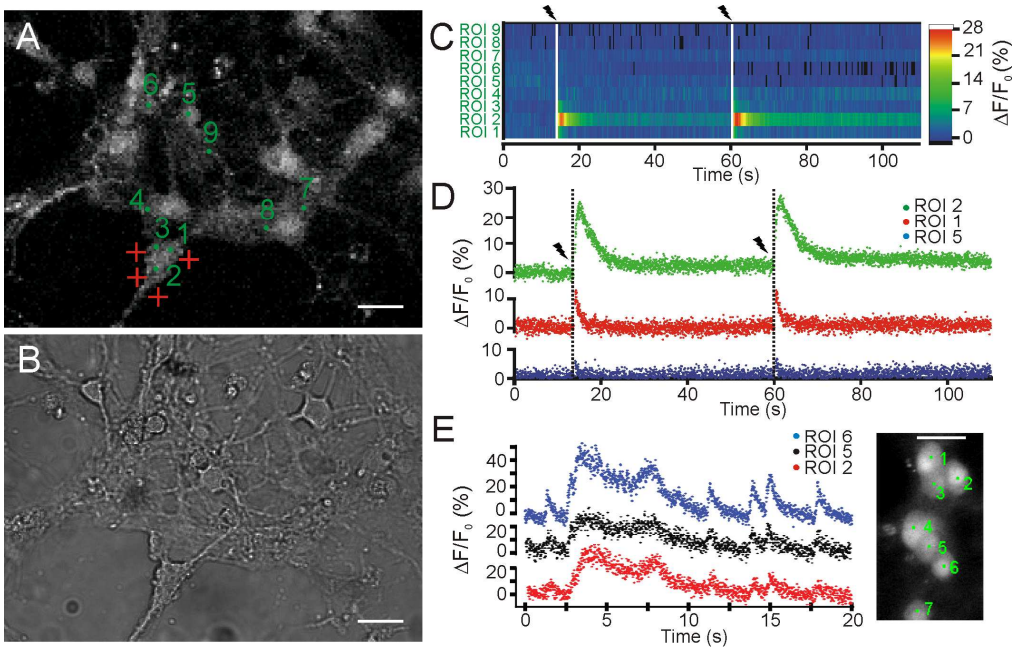

Fig. 5. Simultaneous holographic imaging and galvo-steered uncaging on living neurons. A) Fluorescence image of Fluo-4-loaded hippocampal neurons in culture. Based on this image, ROIs corresponding to different cells or portion of a given cell are identified (green spots numbered 1-9). These ROIs are used to generate a phase hologram which results in fluorescence imaging over time only in those ROIs. The location of the four uncaging spots is indicated by the red crosses. Scale bar: 20 μm. (B) Transmitted light image of the same field of view shown in A. Scale bar: 20 μm. (C) $\Delta F/F_0$ values of Fluo-4 fluorescence as a function of time for the nine regions of interest before and after the sequential uncaging of MNI-glutamate in four different locations (red crosses in A). The arrows indicate the time of delivery of the photolysis stimulus. (D) The fluorescence time course in three different regions is shown. Note that in ROI #1-2, but not ROI #5, a clear response to MNI-glutamate uncaging is observed. (E) Left: Time course of Fluo-4 fluorescence for three holographic dots showing spontaneous Ca^{2+} signals recorded at 71 frames/s. The position of the different ROIs is shown in the fluorescence image displayed on the right. Scale bar 15 μm.

In the experiment shown in Fig. 5C-D, imaging was performed at 30 frames/s which is more than sufficient to follow the relatively slow dynamics of the calcium signals. It should be noted however, that in this experimental configuration the acquisition speed can be further increased and is conceptually limited only by the camera acquisition frequency. Nonetheless, the number of frames per second was experimentally limited by the necessity to efficiently excite the fluorophore of interest thus resulting in a sufficiently high signal-to-noise ratio. For example, we routinely recorded spontaneous Ca^{2+} signals by imaging simultaneously multiple spots in the field of view at > 70 frames/s (Fig. 5E).

The time course of the $\Delta F/F_0$ Fluo-4 fluorescence for the nine ROIs is shown in Fig. 5C. When MNI-glutamate (1.5 mM) was photolysed by a sequence of four laser pulses onto an identified cell (red spots in Fig. 5A; single pulse duration of the uncaging beam, 1 ms; laser power, 7 mW; λ = 720 nm), a large Ca^{2+} response limited to the stimulated cell could be observed. Repetition of the same stimulus after a few tens of seconds resulted in similar Ca^{2+} responses. In control experiments, when MNI-glutamate was not present in the extracellular solution, the same stimuli resulted in no change in Fluo-4 fluorescence.

We then tested our holographic microscope in the configuration described in Fig. 1B. Full field images of Fluo-4 fluorescence were acquired with the imaging beam using conventional two-photon scanning microscopy at 0.54 Hz. Based on the Fluo-4 fluorescence signal, different regions of the field of view corresponding to two cell somata (white areas in Fig. 6C)

#128503 - $15.00 USD Received 26 May 2010; revised 29 Jul 2010; accepted 7 Aug 2010; published 18 Aug 2010

were selected and used to generate holographic photolysis only in those specific areas (regions delimited by red lines in Fig. 6D).

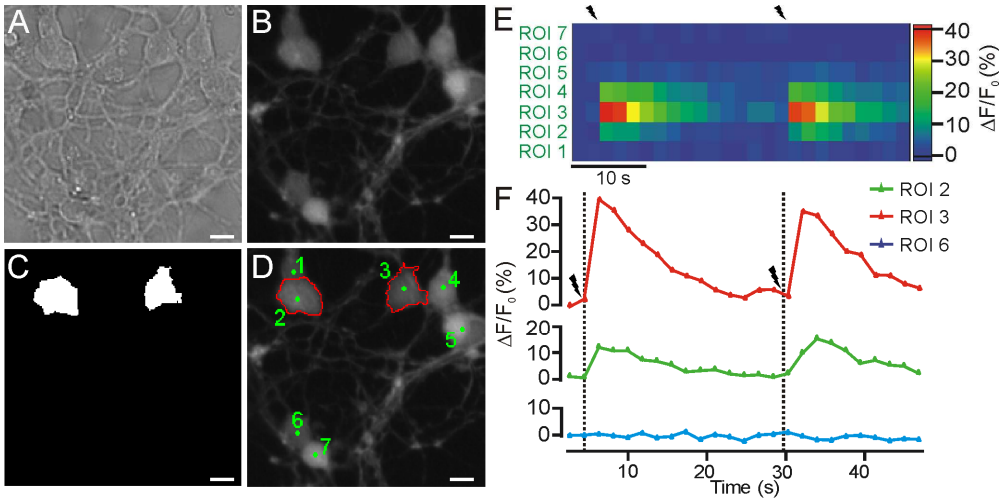

Fig. 6. Simultaneous scanning fluorescence imaging and holographic uncaging. A) Bright field image of cerebellar granule cells in culture. Scale bar: 10 µm. (B) Epifluorescence image displaying Fluo-4 loaded neurons in the same field of view shown in A). Based on this image, an image mask (C) is generated to shape the laser wave front of the uncaging beam. (D) While uncaging is performed simultaneously on two identified cells (areas delimited by red lines), imaging is performed with conventional scanning microscopy at 0.54 Hz. ROIs (numbered from 1 to 7) corresponding to different cells are shown in green. E-F) Time course of $\Delta F/F_0$ values of Fluo-4 fluorescence in the 7 ROIs displayed in D) before and after the application of the holographic uncaging stimulus. Note the clear response of the neurons (ROIs #2 and #3) upon which MNI-glutamate was holographically uncaged. The arrows indicate the time of delivery of the photolysis stimulus.

Laser power of the uncaging beam (at 720 nm) was 0.26 mW/µm^2, while the pulse duration was 50 ms. Figure 6E-F show the time course of the $\Delta F/F_0$ Fluo-4 fluorescence in 7 circular ROIs (green spots in Fig. 6D, numbered 1 through 7) before and after holographic photolysis of MNI-glutamate with the illumination pattern shown in Fig. 6C. Ca^{2+} signals in the selected cells (ROI #2 and #3) were observed upon MNI-glutamate uncaging. After the first photolysis event, delivery of a second identical stimulus resulted in similar neuronal responses (Fig. 6E-F). Importantly, in control experiments where MNI-glutamate was absent from the extracellular solution, the same stimulus used to uncage MNI-glutamate had no effect on Fluo-4 signals (data not shown).

4. Discussion

In this study we present a new optical set-up for simultaneous two-photon imaging and uncaging with structured light illumination. The core of our system is the "holographic module", a simple and compact optical path that shapes the Gaussian distribution of the two-photon beam by using a reflective LCOS-SLM. We propose the "holographic module" as an effective add-on to commercial non-linear microscopes for the illumination of biological samples with complex light patterns. We demonstrate that the implementation of a Prairie Ultima IV scanhead with the "holographic module" results in a flexible optical systems with two main experimental configurations for simultaneous two-photon imaging, uncaging and holography. In the first configuration, fast holographic imaging combined with point uncaging can be performed; in the second, conventional scanning imaging is combined with holographic uncaging. Both configurations were tested to study Ca^{2+} responses in living neurons following caged-glutamate photolysis, proving the potential of this new optical

#128503 - $15.00 USD Received 26 May 2010; revised 29 Jul 2010; accepted 7 Aug 2010; published 18 Aug 2010

system for the study of neuronal function with holographic illumination generated by a LCOS-SLM.

Besides the use of LCOS-SLMs, different experimental strategies have been introduced for illuminating biological samples with complex light patterns. These approaches include digital micromirror devices (DMDs) [3], multibeam illumination [4] and acusto optic deflectors (AODs) [5]. LCOS-SLM technology presents advantages with respect to DMDs as the latter modulates the amplitude and not the phase of the incident beam, thus leading to significant power loss. Moreover, unlike DMDs, the DOE generated with LCOS-SLMs make use of the whole numerical aperture of the objective and may allow the simultaneous illumination of distinct regions of interest at different axial positions [17–19]. Illumination of the sample with multiple beams impinging on the back-aperture of the objective with different angles can provide simultaneous monitoring of multiple regions of interest (ROIs) in the field of view [20]. Nonetheless, given that any ROI requires the design of a specific optical path, it is clear that this approach is limited to a small number of ROIs and does not offer the flexibility of the LCOS-SLM in shaping the laser light to a desired pattern. On the other hand, LCOS-SLMs present advantages also when compared with AODs. LCOS-SLMs allow the simultaneous illumination of different portion of the field of view while AODs steer the laser beam needing a few microseconds to travel from one position to the other. Moreover, AODs allow fast positioning, but not shaping, of the laser beam and usually require pre-chirping. Altogether LCOS-SLMs represent a valid and relatively inexpensive approach for sculpting two-photon illumination.

It is important to note that, in order to holographically illuminate specific regions of a biological sample with high precision in light localization, it is necessary to couple the holographic path with a high resolution imaging system such as a confocal or HiLo microscopes [12]. By using non-linear excitation, our approach takes advantage of the intrinsic “confocality” of two-photon excitation to acquire thin optical sections of the sample for the generation of our DOEs without the need for image processing.

There are different ways to further improve the optical design of our microscope. In the experiments presented in this paper, we used 830 nm laser light for imaging and 720 nm laser illumination for uncaging, but in principle any wavelength in the tunable range of the two laser sources (680-1080 nm for the Chameleon, Ultra II, Coherent) can be used on either one of the optical paths. If different wavelengths are needed, only the combining dichroic mirror (DM0 in Fig. 1) has to be changed. This requires a set of dichroic mirrors with different cut-off wavelengths to match those used experimentally. As a potential alternative solution, DM0 could be replaced by a polarizing beam splitter. Given that the holographic beam is polarized in the horizontal plane, a half-wave plate could be placed in the non-holographic beam and rotated to obtain light polarized in the plane perpendicular to that of the holographic beam. An additional possibility is the use a 50:50 beam splitter which, nonetheless, would result in a 50% net power loss on either beams. Both options would give the flexibility of working with any wavelength in the tunable range of the two laser sources without the need of changing the dichroic DM0. This is going to be particularly useful when, for example, photostimulation requires longer wavelengths than imaging. An additional improvement would regard the “holographic module” which could be easily duplicated allowing the simultaneous sculpting of the laser wavefront on both the imaging and the uncaging beams.

While optical approaches have proved to be a fundamental tool for the study of brain function, the possibility to simultaneously illuminate multiple regions of a field of view with complex shapes promises to bring the optical investigation of neuronal networks to its next level of complexity. The diffusion of optical set-ups that allow spatial shaping of laser light is, however, still very limited in experimental Neuroscience. The microscope described herein is unique in combining two-photon imaging and uncaging with holography. The core of our system, the “holographic module”, is designed to be a compact, plug-in optical path that can be easily implemented on commercial scanning microscopes. This system can be used for

#128503 - $15.00 USD Received 26 May 2010; revised 29 Jul 2010; accepted 7 Aug 2010; published 18 Aug 2010

simultaneous scanning imaging of Ca^{2+} dyes and holographic photostimulation of opsins, caged compounds or photo-switchable proteins leading to fundamental advancements in our understanding of neuronal network function at cellular and subcellular resolution. At the same time, the present microscope will allow fast, fluorescence imaging with two-photon excitation in user-defined regions of interest and in combination with spot uncaging. These applications, together with the observation that two-photon light penetrates deeper in biological tissue and that some opsins are excitable at two-photon, open new perspectives in the use of the present technology for *in vivo* studies.

Acknowledgments

We thank F. Succol for cell culture preparation and the Group of Optics, Department of Physics, Glasgow University for the freeware software. We are grateful to D. Cojoc, A. Diaspro, E. Di Fabrizio and M. Szulczewski, for critical reading of and helpful comments on the manuscript. This work was supported by grants from MIUR PRIN program to F. Benfenati, Telethon-Italy (GGP09134 to F. Benfenati and GGP10138 to T. Fellin) and by the San Paolo "Programma in Neuroscienze" grant to F. Benfenati and T. Fellin. M. Dal Maschio and F. Difato contributed equally to this work.

#128503 - $15.00 USD Received 26 May 2010; revised 29 Jul 2010; accepted 7 Aug 2010; published 18 Aug 2010